N95- 17288

TDA Progress Report 42-119 November 15, 1994

Antenna Noise Temperatures of the 34-Meter Beam-Waveguide Antenna With Horns of Different Gains Installed at F1

T. Y. Otoshi, P. R. Lee, and M. M. Franco
Ground Antennas and Facilities Engineering Section

This article presents a set of theoretical and measured zenith-antenna noise temperatures at 8.45 GHz for the DSS-13 34-m beam-waveguide antenna when horns of different gains are installed at F1. The methodology for calculations is shown in detail. The major differences between calculated and measured values are attributed to changes in subreflector support leg scattering when illuminated by the various horns.

I. Introduction

A study program was initiated to find causes of higher than expected noise temperatures measured at three focal points in a beam-waveguide (BWG) antenna system. The program consists of developing theoretical models for making predictions and obtaining experimental data for model verifications. Theoretical methods are being developed to predict noise temperatures at focal points F1, F2, and F3. Focal point F1 is the Cassegrain focal point near the main reflector vertex. An intermediate focal point F2 lies above the azimuth track, and focal point F3 is the final BWG focal point, located in a subterranean pedestal room. Degradations caused by the BWG system mirrors and shrouds were experimentally determined from comparisons made of values measured at the different focal points [1].

The purpose of this article is to present theoretical and measured zenith-antenna noise temperature values at 8.45 GHz for the DSS-13 34-m BWG antenna with different horns installed at F1. The horns are corrugated, each horn having the same 6.25-deg semiflare angle but of different lengths and aperture diameters.

II. Analytical Procedure and Results

The calculation methodology differs from others used previously in that (1) the noise temperature generated by the horn spillover (into the sky regions) between the edges of the subreflector and main reflector is taken into account, (2) subreflector and main reflector efficiencies (to be defined) are applied as necessary in the calculations of noise temperature contributions, and (3) brightness temperatures are computed for each theta for horn, subreflector, and main reflector radiation patterns for the weather conditions that prevailed at the time of the experiments.

A. Radiation Patterns and Spillover Power Ratios

Table 1 is a summary of the power ratios of the subreflector forward spillover, the main reflector spillover towards ground, and the spillover into the BWG opening on the main reflector. These power ratios were obtained by first calculating horn patterns at the frequency of 8.45 GHz using the circular waveguide mode matching program CWG.F [2]. The term "horn gain" used throughout this article is the directivity of the horn calculated from these patterns. The radiation pattern from the subreflector for each incident horn pattern was then calculated for eight phi-plane cuts with the physical optics program POSUB.F. Next, the spherical wave azimuthal expansion program AZEXP.F was used to integrate the total power in the radiation pattern. The total power was then normalized and subtracted from the horn input power to obtain the subreflector spillover power ratio.

Main reflector spillover towards ground was obtained by using a radiation pattern from the subreflector calculated at a near-field radius of 1780.5 cm, the distance to the outer edge of the main reflector (see Fig. 1). This pattern was used as input into the programs AZEXP.F and EFFIC.F to calculate the fraction of the power in the radiation pattern incident between the edge of the main reflector surface and the horizon. Spillover into the BWG opening of 243.8-cm diameter was calculated similarly, using a radiation pattern from the subreflector calculated at a near-field radius of 1191.3 cm, the distance to the edge of the BWG opening. In addition, Table 1 shows the spillover into the total BWG opening of the 304.8-cm diameter, which includes the Cassegrain cone mounting ring. However, since this mounting ring reflects power to the sky, only the spillover into the actual opening (determined by the 243.8-cm diameter of the BWG shroud walls) will be considered for noise temperature analyses.

For purposes of determining noise temperature contributions due to radiation of reflected power from the main reflector into the far field, antenna patterns and beam efficiencies were obtained for the 34-m-diameter main reflector when illuminated by the subreflector patterns for the various horn-gain cases. Figure 2 shows the far-field radiation patterns for the 34-m BWG antenna for the 29.7-dBi and the 22.5-dBi horn-gain cases. The patterns for the other intermediate horn-gain cases fall somewhere between the patterns for these largest and smallest aperture diameters. As an example, see Fig. 3. These patterns were obtained by using the calculated horn patterns as input to the program POJB.F, which is a physical optics program developed by the Ground Antennas and Facilities Engineering Section. The shapes of the patterns are approximately $J_1(u)/u$, where u is related to theta [3].

Table 2 shows the far-field gains of the BWG antenna at 8.45 GHz for the various horn-gain cases. The gain includes only the losses from the main reflector spillover and the subreflector spillover, and the illumination loss at the main reflector aperture. The actual gain would be lower due to any resistive losses in the horn, subreflector, and main reflector surfaces. Beam efficiencies are tabulated for theta at 0.5 and 1.0 deg for the various horn-gain cases.

B. Antenna Noise Temperature Contributions

For calculations of antenna noise temperature contributions, it is important that power ratios be multiplied by the subreflector and main reflector efficiencies defined in Appendix A. Use of the correct power ratios is a necessary step that must be taken to preserve the conservation of power principle in noise temperature calculations [4]. In Appendix A, it is shown that the requirement is met because the sum of all fractional powers involved in the overall noise temperature calculations is equal to unity.

Table 3 shows a summary of the calculated zenith antenna noise temperature contributions for the 34-m BWG antenna for the various horn-gain cases. Supporting data as well as the calculation methodologies used to obtain these final values may be found in Appendix A.

To compute horn contributions, the brightness temperatures and horn beam efficiencies were first computed from TYO61M4A, which is a FORTRAN program similar to that described in [5]. Then noise temperature contributions from the horn patterns in the sky region (between subreflector and main

Table 1. Predicted F1 spillover amounts, 8.45 GHz, physical optics analysis.[a]

Horn diameter, cm (in.)	Horn gain, dBi	p_{S1} (subreflector spillover)	p_{S2} (main reflector spill to ground)	p_{S3} (spill into 304.8-cm BWG opening)	p_{S3} (spill into 243.8-cm BWG opening)
48.346 (19.034)	29.71	0.0294	0.0022	0.0039	0.0023
40.754 (16.045)	28.70	0.0503	0.0030	0.0031	0.0018
31.458 (12.385)	26.90	0.0827	0.0036	0.0020	0.0012
24.948 (9.822)	25.12	0.1465	0.0082	0.0014	0.00086
17.976 (7.077)	22.52	0.3437	0.0149	0.0010	0.00057

[a] See Appendix A for further definitions of p_S symbols.

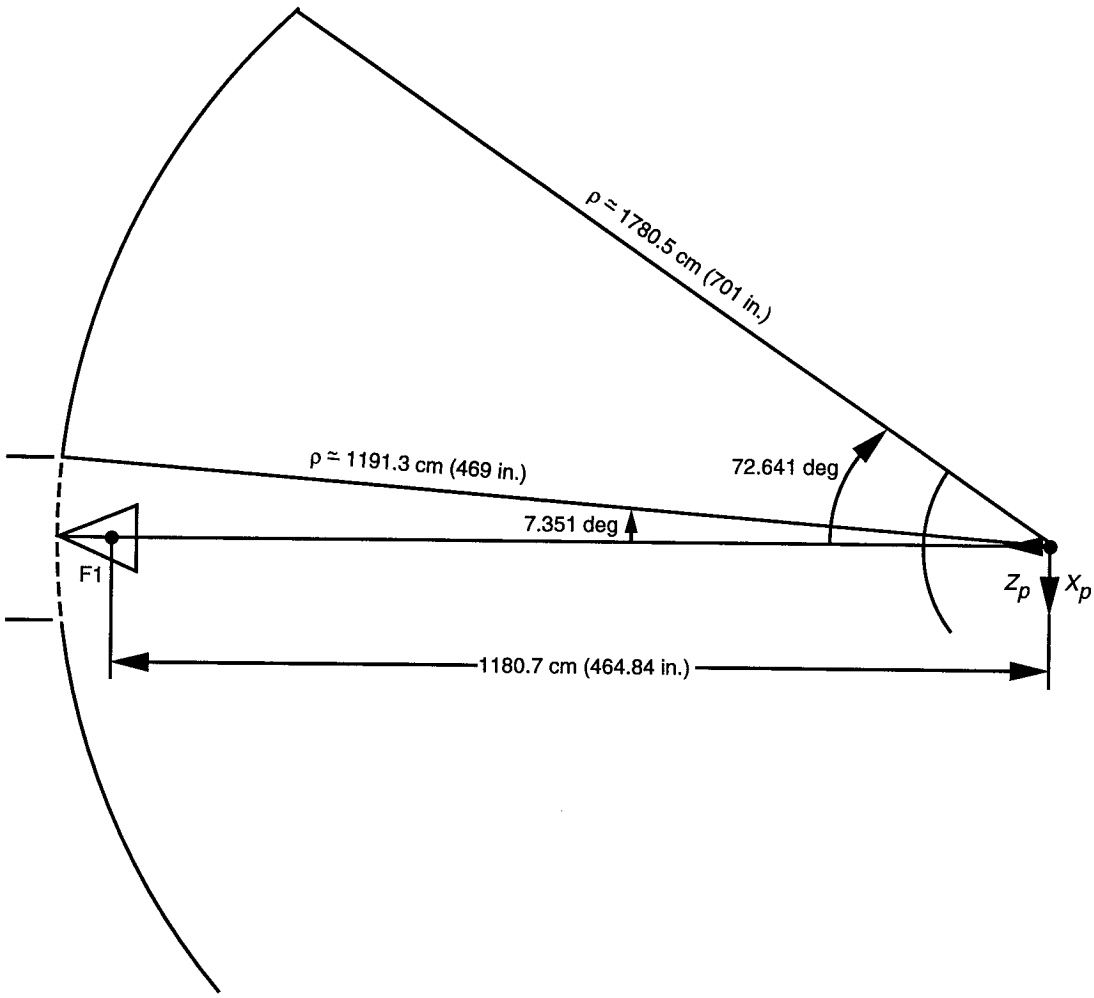

Fig. 1. Geometry for calculating the main reflector and BWG opening contribution using the POSUB.F program.

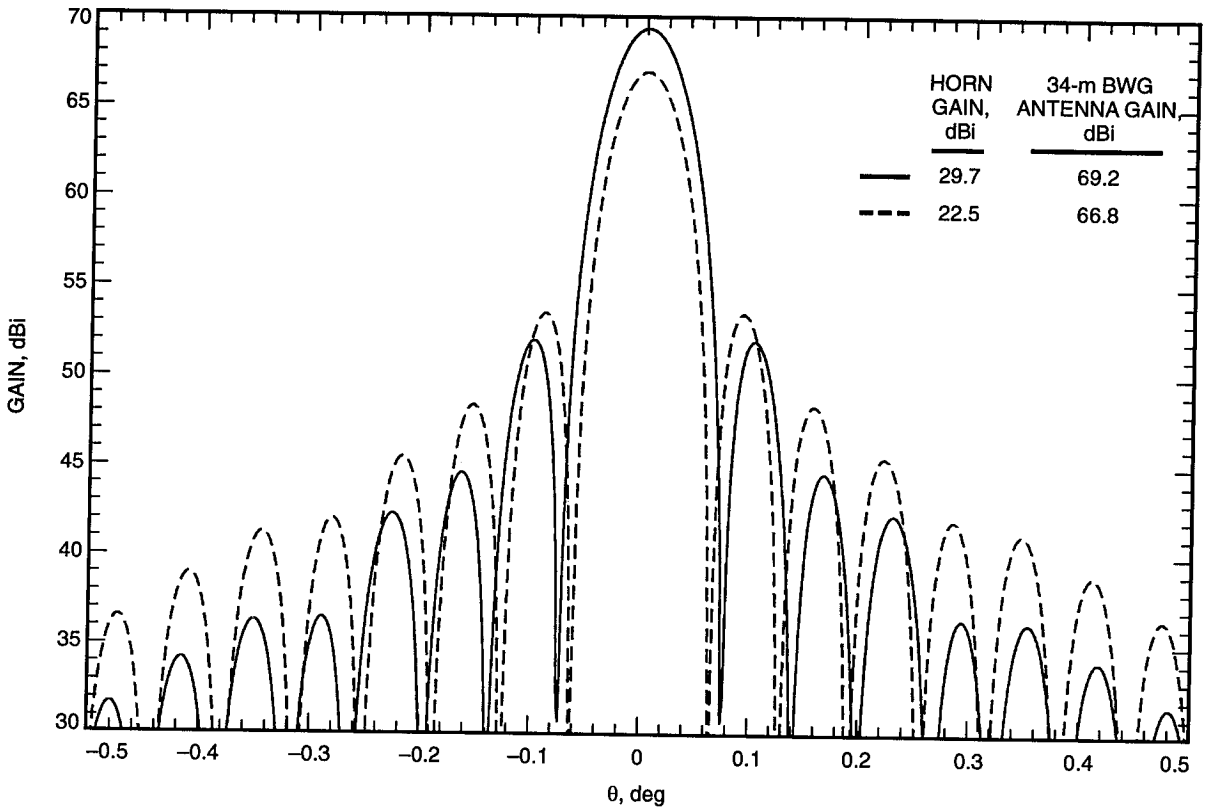

Fig. 2. The 34-m BWG antenna far-field patterns and gain at 8.45 GHz for the largest and smallest aperture horn at F1.

Table 2. Far-field data for the 34-m-diameter antenna at 8.450 GHz for various horns at F1.

Horn gain, dBi	34-m-diameter antenna			
	Gain, dBi	First null, deg	Beam efficiency	
			At 0.5 deg	At 1.0 deg
29.71	69.21	0.075	0.9909	0.9982
28.70	69.10	0.073	0.9921[a]	0.9988[a]
26.90	68.83	0.069	0.9838	0.9973
25.12	68.28	0.066	0.9704	0.9939
22.52	66.80	0.063	0.9567	0.9907

[a] The efficiencies at 0.5 deg and 1.0 deg are slightly larger for the 28.7-dBi horn than those for the 29.7-dBi horn. This is attributed to slight differences in the main-lobe beamwidths and the close-in sidelobe patterns. These differences affect the power contained inside the patterns up to the arbitrary 0.5-deg and 1.0-deg angles selected.

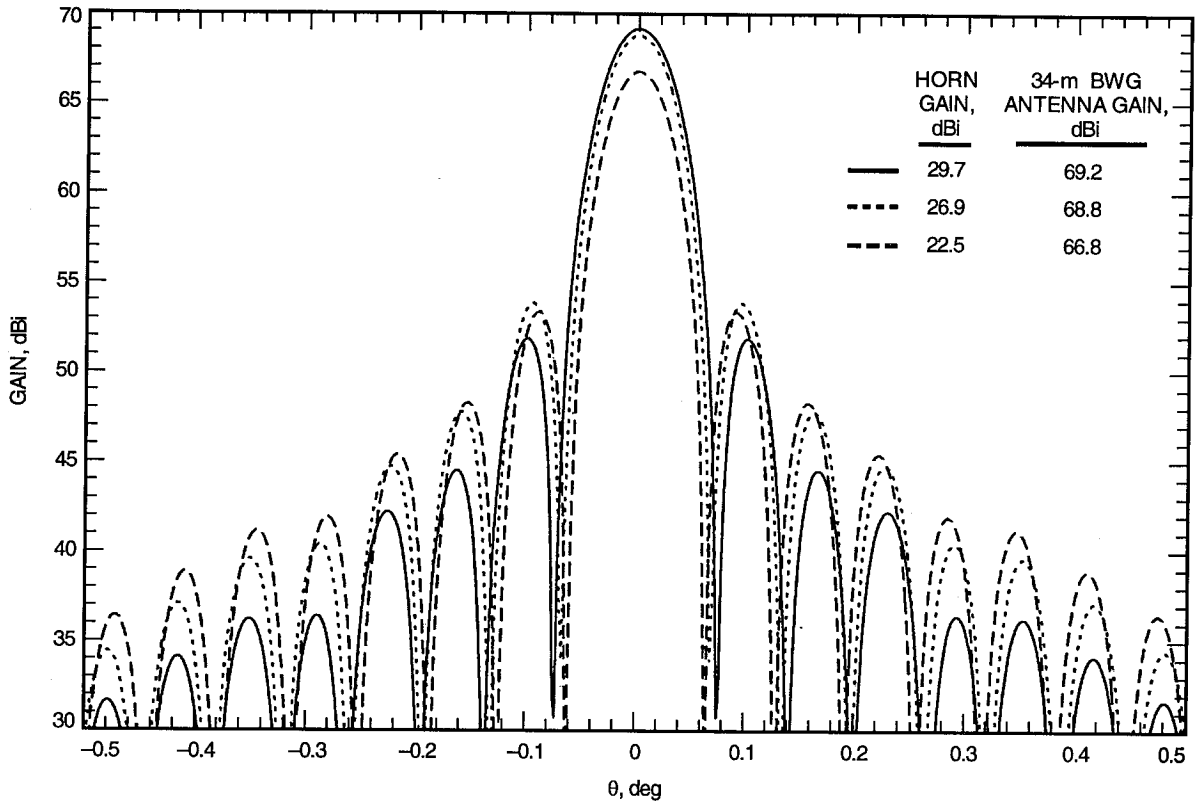

Fig. 3. The patterns of Fig. 2 in addition to the pattern for an intermediate-sized horn aperture.

Table 3. Summary of antenna noise temperature contributions at F1.[a]

Horn gain, dBi	ΔT_{A1} (main reflector to zenith), K	ΔT_{A2} (subreflector to sky/ground), K	ΔT_{A3} (subreflector to BWG hole), K	ΔT_{A4} (horn to sky, 8.7 to 68.2 deg), K	ΔT_{A5} (horn to other spills), K	$\sum_{i=1}^{5} \Delta T_{Ai}$, K	Noise temperature difference, K
29.7	4.370	0.455	0.657	0.121	0.018	5.621	—
28.7	4.263	0.595	0.510	0.194	0.046	5.608	−0.01
26.9	4.125	0.706	0.329	0.307	0.094	5.561	−0.06
25.1	3.826	1.471	0.210	0.564	0.140	6.211	0.59
22.5	2.919	2.059	0.120	1.396	0.232	6.726	1.11

[a] See Appendix A for details.

reflector edges) were determined from the program output. A sample case output of this program is included in Appendix B.

Next, as discussed in Section II.A, from the spillover power ratios computed for the region outside the outer edge of the main reflector, the noise temperature contribution was determined by first determining an effective brightness temperature of the ground and low-horizon sky region. Due to the variability of this region with changes in weather and ambient temperature as well as zenith angle, the brightness

temperatures were calculated for the applicable conditions that existed during the corresponding measurement periods. The effective brightness temperatures were obtained through the use of a BASIC program named SREFLNT.BAS. A sample case output may be seen in Appendix B. Effective brightness temperatures for this ground and low-horizon sky region may be seen in Table A-3. It is of interest that these effective brightness temperatures vary from 210 K to 217 K, as contrasted with the 240-K value that has been used at JPL in past years for these types of calculations for Cassegrain antennas.

The BWG opening noise contribution is computed from the power ratio values and equations given in Appendix A. Since the Cassegrain mounting ring surface will reflect power into the sky close to zenith, only the 243.8-cm-diameter portion of the BWG shroud opening should contribute significantly to the antenna noise temperature at F1. Noise temperature calculations are shown in Table A-4. The brightness temperature of the shroud opening was assumed to be equal to the ambient temperature of the antenna at the times that system noise temperature measurements were being performed for corresponding horn configurations.

To determine the contribution due to sky absorption of the power radiated by the main reflector, it was necessary to compute beam efficiencies as a function of zenith angle for the various horn-gain cases. These values as tabulated in Table 2 show that, for all horn-gain cases, 99 percent of the power radiated by the main reflector will be contained inside the main beam between 0 deg and 1 deg of zenith θ angles. Since sky brightness temperature is nearly constant (within 1.5 percent) from 0 to 10 deg of zenith angle, it can be assumed that, for these theoretical cases, 100 percent of the power radiated from the 34-m BWG main reflector surface will be absorbed by sky that has an effective brightness temperature equal to that at the zenith angle of 0 deg. It should be pointed out that the brightness temperature of the zenith sky, as calculated from program TY061M4A, includes the cosmic background and atmospheric loss contributions (see Appendix B).

Table 3 shows most of the contributions to antenna noise temperatures. If the total absolute antenna noise temperatures need to be computed, then knowledge is also required of such additional terms as noise due to tripod scattering of the far-field plane wave illuminating the entire antenna, main reflector panel leakage, main reflector and subreflector resistive losses, and other terms presented in [6]. It will be shown later in this article that this residual term is approximately equal to 3.0 K.

III. Experimental Work

Operating noise temperature measurements were sequentially made at 8.450 GHz with the phase centers of the 29.7-, 28.7-, 26.9-, 25.1-, and 22.5-dBi horns aligned with the geometric focal point F1. Figure 4 shows the experimental test setup of the 29.7-dBi horn at F1.

The experimental data are presented in Tables 4 and 5. In Table 4,

$$\Delta T_{op1} = L_{wg}[T_{op} - (T_{op})_{ref}] \tag{1}$$

where $(T_{op})_{ref}$ is the normalized operating noise temperature of the 29.7-dBi horn, and L_{wg} is the waveguide loss from the horn apertures to the high-electron-mobility-transistor (HEMT) input. It was assumed that L_{wg} measured for the 22.5-dBi horn [1] applied to all horn-gain cases.

To experimentally determine only the noise temperature contribution from spillover into the 243.8-cm-diameter BWG opening at F1 below the feedhorn, a ground plane was installed below the feedhorns. Figure 5 shows the installation of a Thermax[1] ground plane below the 29.7-dBi horn. The

[1] A trademark of the Celotex Corporation, Tampa, Florida.

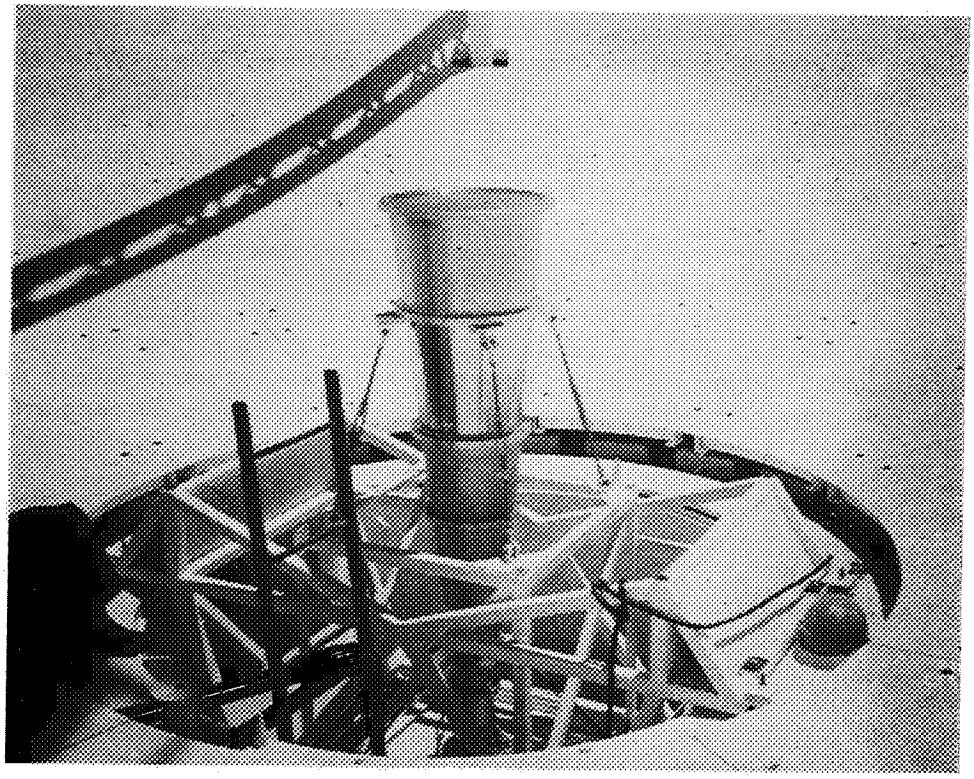

Fig. 4. Partial view of the X-band 29-dBi horn test package and mounting structure installed at the Cassegrain focal point F1.

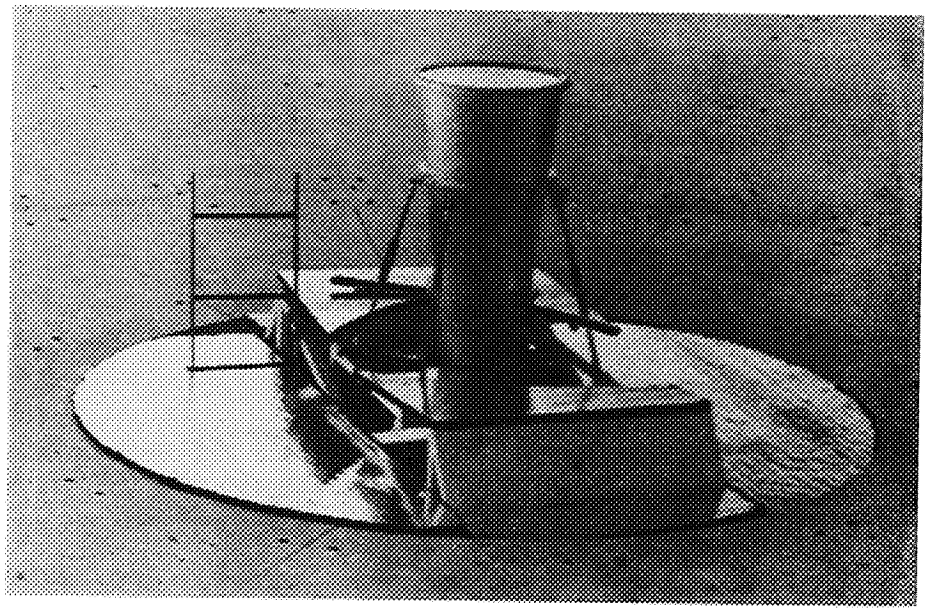

Fig. 5. The installation shown in Fig. 4 with the addition of a Thermax™ ground plane that covers the 243.8-cm-diameter BWG opening below the feedhorn.

Table 4. DSS-13 measured and normalized noise temperature (T_{op}) without a Thermax™ conducting plane below the feedhorn at F1.[a]

Horn gain, dBi	Horn phase center,[b] cm	Relative humidity, percent	Temperature, deg C		Barometric pressure, mb	T_{op}, K		Measured ΔT_{op1},[e] K
			Load	Outdoor		Measured[c]	Normalized[d]	
29.7	116.8	5.00	28.56	25.47	896.88	27.08	27.07	0.00
28.7	82.6	4.42	28.43	26.90	895.80	27.13	27.14	0.05
26.9	44.5	5.01	28.80	25.62	895.59	27.12	27.12	0.04
25.1	25.4	5.17	29.60	26.67	895.30	28.07	28.04	1.01
22.5	7.9	4.92	29.97	26.79	894.99	29.03	29.00	1.98

[a] Frequency = 8.45 GHz.
[b] Phase center location is measured down from the horn aperture.
[c] Data were taken with the research and development (R&D) X-band test package described in [1]. L_{wg} = 1.0163 (0.07 dB).
[d] Normalized T_{op} corrected for standard atmosphere and waveguide ambient temperature [1].
[e] See Eq. (1).

Table 5. DSS-13 measured and normalized noise temperature (T_{op}) with a Thermax™ conducting plane below the feedhorn.[a]

Horn gain, dBi	Horn phase center,[b] cm	Relative humidity, percent	Temperature, deg C		Barometric pressure, mb	T_{op}, K		Measured ΔT_{op2},[e] K
			Load	Outdoor		Measured[c]	Normalized[d]	
29.7	116.8	5.35	27.95	24.87	896.99	26.67	26.67	0.41
28.7	82.6	4.33	28.28	26.39	895.59	26.74	26.76	0.39
26.9	44.5	5.17	28.73	25.81	895.59	26.83	26.82	0.31
25.1	25.4	5.04	29.76	26.59	895.29	27.80	27.78	0.26
22.5	7.9	4.93	29.92	27.07	894.99	28.74	28.71	0.30

[a] Frequency = 8.45 GHz.
[b] Phase center location is measured down from the horn aperture.
[c] Data were taken with the R&D X-band test package described in [1]. L_{wg} = 1.0163 (0.07 dB).
[d] Normalized T_{op} corrected for standard atmosphere and waveguide ambient temperature [1].
[e] See Eq. (2).

last column of Table 5 shows the change in T_{op} values measured with and without the Thermax™ ground plane. The values were computed from

$$\Delta T_{op2} = L_{wg}[(T_{op})_{w/o} - (T_{op})_{with}] \tag{2}$$

This difference provides a measured value of the noise contribution due to spillover into the 243.8-cm-diameter BWG opening at F1, and the difference is compared to the theoretical ΔT_{A3} values shown in Table 3.

IV. Discussion of Results

The zenith T_{op} value of the 34-m BWG antenna with the X-band test package and a particular feedhorn installed at F1 can be expressed as

$$(T_{op})_{F1} = L_{wg}^{-1} T_{A,F1} + T_{wg} + T_{hemt} + T_{fu} \tag{3}$$

where $T_{A,F1}$ is the 34-m BWG antenna noise temperature at F1 and the other symbols are defined in Appendix A. Algebraic manipulation of Eq. (3) gives

$$T_{A,F1} = (T_{op})_{F1} - L_{wg}(T_{wg} + T_{hemt} + T_{fu}) \tag{4}$$

From [1], $L_{wg} = 1.0163$, $T_{wg} = 4.69$ K, $T_{hemt} = 13.0$ K, and $T_{fu} = 0.4$ K, and from Table 4, the measured $(T_{op})_{F1}$ for the 29.7-dBi horn is shown to be 27.08 K. Substitution of these values in Eq. (4) gives

$$T_{A,F1} = 8.70 \text{ K}$$

which includes the cosmic background and atmospheric loss contributions. It is also valid to state that

$$T_{A,F1} = \sum_{i=1}^{5} \Delta T_{Ai} + T_u \tag{5}$$

which gives

$$T_u = T_{A,F1} - \sum_{i=1}^{5} \Delta T_{Ai} \tag{6}$$

where T_u is a residual (currently unknown) contribution due to strut scattering, leakage through gaps in the main reflector surface, holes in the main reflector surface panels, and subreflector and main reflector resistive losses. Some of the values for these contributions can be obtained from [6].

Substitution of $T_{A,F1} = 8.70$ K and $\sum_{i=1}^{5} \Delta T_{Ai} = 5.62$ K (from Table 3) in Eq. (6) gives

$$T_u = 3.08 \text{ K}$$

Another method of getting an approximate value for T_u is from the relationship

$$(T_u)_{approx} = (T_{op})_{F1} - (T_{op})_{ground} \tag{7}$$

where $(T_{op})_{ground}$ is the operating noise temperature of the portable front-end X-band test package (with horn) on the ground [1]. The value on the right-hand side of Eq. (7) was shown in [1] to be 3.2 K for the 29.7-dBi horn configuration.

For interest, differential antenna noise temperatures (relative to the 29.7-dBi horn) are presented in Table 6. Values for this table were derived from values given in Tables 3 and 4. The differential values

shown in the last column of Table 6 are attributed primarily to residual tripod (strut) contributions not taken into account correctly by the theoretical method. Tripod contributions are difficult to calculate, but an estimate of the changes can be obtained by first accounting for all known or best-estimate contributions (excluding tripod contributions) and then subtracting the calculated total from the measured value. Note that more noise contribution from the tripod occurs for the horns of smaller gain. As shown in Table 7, horns of smaller gain illuminate more of the tripod legs away from the tripod-subreflector connection points and thus have higher tripod-scatter contributions.

Table 6. Relative differences between antenna temperatures of the 29.7-dBi horn and other horns installed at F1.[a]

Horn gain, dBi	ΔT_A,[b] K		
	Measured[c]	Calculated[d]	Difference
29.7	—	—	—
28.7	0.05	−0.01	0.06
26.9	0.04	−0.06	0.10
25.1	1.01	0.59	0.42
22.5	1.98	1.11	0.87

[a] Frequency = 8.45 GHz.
[b] $\Delta T_A = [(T_A)_{horn} - (T_A)_{29.7\ dBi\ horn}] \approx \Delta T_{op1}$.
[c] From Table 4.
[d] From Table 3.

Table 7. Comparison of fractional powers in scatter regions near the subreflection edge.

Horn gain, dBi	θ_i, deg	Fraction of total power contained in θ_i region
29.7	8.7 to 11	0.0173
	11 to 17	0.0084
28.7	8.7 to 11	0.0291
	11 to 17	0.0121
26.9	8.7 to 11	0.0357
	11 to 17	0.0282
25.1	8.7 to 11	0.0747
	11 to 17	0.0429
22.5	8.7 to 11	0.1533
	11 to 17	0.1293

V. Conclusions

A methodology has been presented for calculating antenna noise temperature contributions of a BWG antenna for various horns placed at Fl. A reference antenna noise temperature is based on the 29.7-dBi horn because this is the equivalent horn for which the BWG antenna was designed. As the

horn gains become smaller towards 22.5 dBi, a larger discrepancy in noise temperature, of about 0.87 K, occurs. This discrepancy is attributed to larger unknown noise contributions from tripod scattering as the horn gain becomes smaller.

References

[1] T. Y. Otoshi, S. R. Stewart, and M. M. Franco, "Portable Microwave Test Packages for Beam-Waveguide Antenna Performance Evaluations," *IEEE Trans. on Microwave Theory and Techniques, Special Issue: Microwaves in Space*, vol. MTT-40, no. 6, pp. 1286–1293, June 1992.

[2] D. Hoppe, "Scattering Matrix Program for Circular Waveguide Junctions," *Cosmic Software Catalog*, 1987 edition, NASA-CR-179669, NTO-17245, NASA's Computer Software Management and Information Center, Athens, Georgia, 1987.

[3] S. Silver, ed., *Microwave Antenna Theory and Design*, Radiation Laboratory Series, New York: McGraw-Hill Book Company, Inc., p. 194, 1949.

[4] W. W. Mumford and E. H. Scheibe, *Noise Performance Factors in Communication Systems*, Dedham, Massachusetts: Horizon House-Microwave, Inc., pp. 16–17 and 20, 1968.

[5] T. Y. Otoshi and C. T. Stelzried, "Antenna Temperature Analysis," *Space Program Summary No. 37-36*, vol. IV, Jet Propulsion Laboratory, Pasadena, California, pp. 262–267, December 31, 1965.

[6] D. A. Bathker, W. Veruttipong, T. Y. Otoshi, and P. W. Cramer, Jr., "Beam-Waveguide Antenna Performance Predictions with Comparisons to Experimental Results," *IEEE Trans. on Microwave Theory and Techniques, Special Issue: Microwaves in Space*, vol. MTT-40, no. 6, pp. 1274–1285, June 1992.

Appendix A

Analysis of Antenna Noise Temperature Contributions at F1

I. Nomenclature (See Fig. A-1)

α_{H1} Fraction of the total horn-radiated power that is captured by the subreflector. This term is equal to the subreflector efficiency.

α_{H2} Fraction of the total horn-radiated power that is absorbed by the sky region between the edges of the subreflector and main reflector.

α_{H3} Fraction of the total horn-radiated power that goes into cross-polarization and becomes absorbed primarily by the sky region, between the subreflector edge and the 50-deg elevation angle.

α_{A1} Fraction of the total horn-radiated power that becomes absorbed by the zenith sky after reflections from the subreflector and main reflector.

α_{A2} Fraction of the total horn-radiated power that becomes absorbed by ground and low-horizon sky region outside the main reflector edge after reflection from the subreflector.

α_{A3} Fraction of the total horn-radiated power that becomes absorbed by the environment inside the BWG opening on the main reflector.

η_{SR} Subreflector efficiency.

η_{MR} Main reflector efficiency.

η_B Beam efficiency.

L_{wg} Loss factor for the waveguide between the horn aperture and the input flange of the HEMT, power ratio.

p_{S1} Fraction of the total horn-radiated power not captured by the subreflector.

p_{S2} Fraction of the subreflector reflected power that radiates and becomes absorbed by the region outside the main reflector. Normalization is done with respect to the subreflector power pattern and not with respect to the horn-radiated power.

p_{S3} Fraction of the subreflector reflected power that radiates to the BWG opening on the main reflector. Normalization is done with respect to the subreflector power pattern and not with respect to the horn-radiated power.

$(T_b)_{A1}$ Brightness temperature of the zenith sky, K.

$(\overline{T_b})_{A2}$ Effective brightness temperature of the nonoptical path environment inside the BWG hole opening, K. (Assume ambient temperature environment.)

$(\overline{T_b})_{A3}$ Effective brightness temperature of the ground and low-horizon sky region for spillover past the main reflector edge, K.

$(\overline{T_b})_{H2}$ Effective brightness temperature for the sky region between the subreflector edge and main reflector edge, K.

$(\overline{T_b})_{H3}$ Effective brightness temperature of the cross-polarization environment, K. (Assume $(\overline{T_b})_{H3}$ to be sky at a 50-deg elevation angle.)

T_{fu} Effective noise temperature of the follow-up receiver, K.

T_{hemt} Effective noise temperature of the HEMT as defined at the input flange of the HEMT, K.

T_{op} Operating noise temperature, K.

T_p Physical temperature of absorber (approximately 300 K).

$T_{sky,zen}$ Brightness temperature of zenith sky, including cosmic background and atmospheric contributions, K.

T_u Unknown residual contribution not taken into account by the method presented in this article, K.

T_{wg} Noise temperature due to waveguide loss between the horn aperture and the input flange of the HEMT, K.

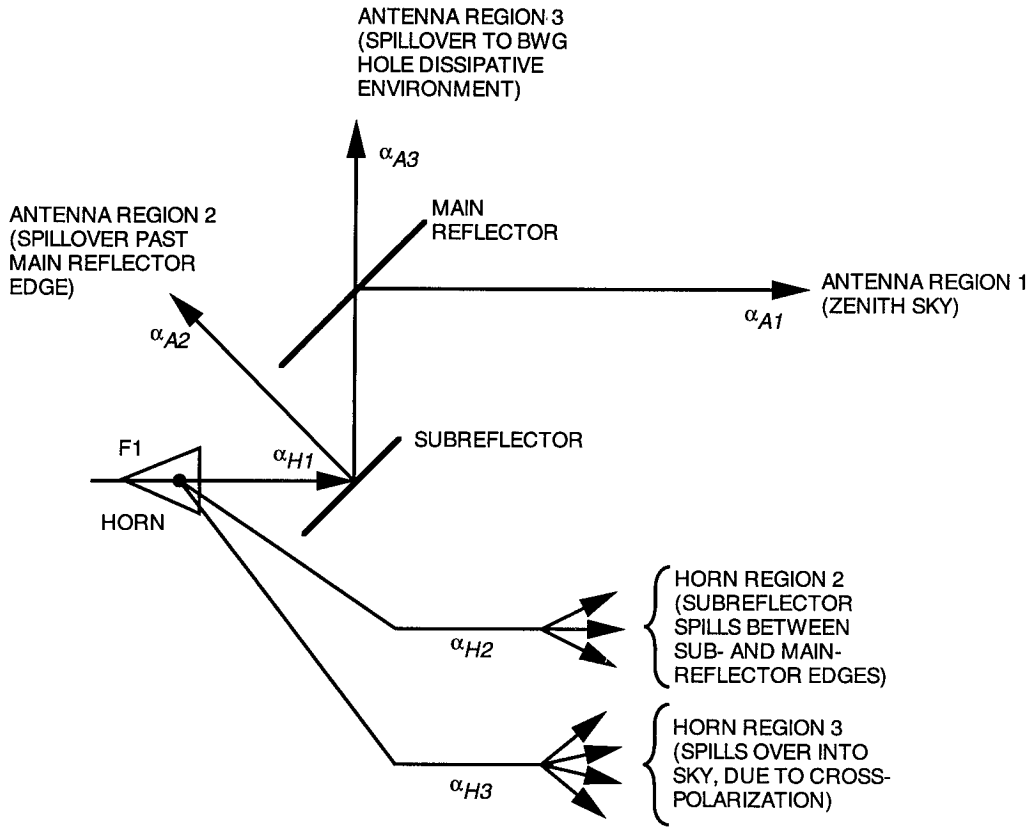

Fig. A-1. Brightness temperature regions contributing to antenna noise temperatures for the horn at F1.

II. Antenna Noise Temperature Contribution Relationships

The following assumptions are made:

(1) The p_{S1}, p_{S2}, and p_{S3} data were obtained from programs discussed in Section II and presented in Table 1.

(2) The α_{H2} data were obtained from Program TYO61M4A, as discussed in Section II.

(3) Normalization of power ratios was done according to the definitions given in Section A-I.

In Fig. A-1, the following relationships hold:

$$\alpha_{H1} = 1 - p_{S1} \;=\; \eta_{SR} \tag{A-1}$$

$$\alpha_{H3} = p_{S1} - \alpha_{H2} \;=\; 1 - \alpha_{H1} - \alpha_{H2} \tag{A-2}$$

$$\eta_{MR} = 1 - p_{S2} - p_{S3} \tag{A-3}$$

$$\alpha_{A1} = \eta_{SR}\eta_{MR} \tag{A-4}$$

$$\alpha_{A2} = p_{S2}\eta_{SR} \;=\; p_{S2}(1 - p_{S1}) \tag{A-5}$$

$$\alpha_{A3} = p_{S3}\eta_{SR} \;=\; p_{S3}(1 - p_{S1}) \tag{A-6}$$

Note that the following conservation of power relationships hold:

$$\alpha_{H1} + \alpha_{H2} + \alpha_{H3} \;=\; 1 \tag{A-7}$$

and since

$$\alpha_{H1} = \alpha_{A1} + \alpha_{A2} + \alpha_{A3} \tag{A-8}$$

then

$$\alpha_{A1} + \alpha_{A2} + \alpha_{A3} + \alpha_{H2} + \alpha_{H3} \;=\; 1 \tag{A-9}$$

The antenna noise temperature contributions are

$$\Delta T_{A1} = \alpha_{A1} T_{sky,zen} \tag{A-10}$$

$$\Delta T_{A2} = \alpha_{A2}(\overline{T_b})_{A2} \tag{A-11}$$

$$\Delta T_{A3} = \alpha_{A3}(\overline{T_b})_{A3} \;=\; \alpha_{A3} T_p \tag{A-12}$$

$$\Delta T_{A4} = \alpha_{H2}(\overline{T_b})_{H2} \tag{A-13}$$

$$\Delta T_{A5} = \alpha_{H3}(\overline{T_b})_{H3} \tag{A-14}$$

The above relations given by Eqs. (A-10) through (A-14) neglect the fact that theoretical patterns do not consider scattering from the tripod subreflector supports that raise the far-out side-lobe levels. Neglecting the tripod–subreflector scattering, the theoretical total antenna noise temperature of the 34-m-diameter antenna at F1 is

$$T_A = \sum_{i=1}^{5} \Delta T_{Ai} + T_u \tag{A-15}$$

where T_u is other unknown contributions from panel leakage, resistive subreflector and main reflector losses, and tripod-scattering effects. As discussed in Section IV, an approximate value of T_u can be obtained from calculated values using the methodology given in [1] or from the measured value of

$$(T_u)_{approx} = (T_{op})_{F1} - (T_{op})_{ground} \tag{A-16}$$

In a future more rigorous analysis, some of the fractional powers associated with T_u might be calculable and then taken into account by including a new term, α_{A4}, in the power ratio relationships given in Eqs. (A-8) and (A-9).

III. Calculated Contributions to Antenna Temperature at 8.450 GHz

Tables A-1 through A-6 are tabulations of calculated antenna temperature contributions for the regions shown in Fig. A-1.

Table A-1. Tabulation of fractional powers and efficiencies at 8.45 GHz.[a]

Horn gain, dBi	$\alpha_{H1} = \eta_{SR}$	α_{H2}[b]	α_{H3}	η_{MR}[c]	α_{A1}	α_{A2}	α_{A3}
29.7	0.9706	0.0264	0.0030	0.9955	0.9662	0.0021	0.0022
28.7	0.9497	0.0427	0.0076	0.9952	0.9451	0.0028	0.0017
26.9	0.9173	0.0671	0.0156	0.9952	0.9129	0.0033	0.0011
25.1	0.8535	0.1231	0.0234	0.9909	0.8457	0.0070	0.0007
22.5	0.6563	0.3051	0.0386	0.9845	0.6461	0.0098	0.0004

[a] See Eqs. (A-1) through (A-6) and Table 1 p_S values for calculation of values presented in this table.
[b] The α_{H2} values were obtained from Program TYO61M4A. See Table A-5.
[c] Use data for the 243.8-cm-diameter BWG opening.

Table A-2. Antenna region 1 contributions (shown in Fig. A-1).

Horn gain, dBi	Average temperature, deg C	Relative humidity, percent	T_{pg},[a] K	$(T_b)_{A1}$,[b] K	α_{A1} (see Table A-1)	ΔT_{A1}, K (see Eq. (A-10))
29.7	25.47	5.00	298.6	4.523	0.9662	4.370
28.7	26.90	4.42	300.1	4.511	0.9451	4.263
26.9	25.62	5.01	298.8	4.519	0.9129	4.125
25.1	26.67	5.17	299.8	4.524	0.8457	3.826
22.5	26.79	4.92	300.0	4.518	0.6461	2.919

[a] Ground level air temperature.
[b] $(T_b)_{A1} = T_{sky}$ looking at zenith, K. Obtain values from TYO61M4A.

Table A-3. Contributions from antenna region 2 (shown in Fig. A-1).

Horn gain, dBi	α_{A2} (see Table A-1)	$(\overline{T_b})_{A2}$,[a] K	ΔT_{A2},[b] K
29.7	0.0021	216.7	0.455
28.7	0.0028	212.5	0.595
26.9	0.0033	213.9	0.706
25.1	0.0070	210.1	1.471
22.5	0.0098	210.1	2.059

[a] $(\overline{T_b})_{A2}$ is derived by dividing ΔT_{A2} by α_{A2}.
[b] ΔT_{A2} is obtained from Program SREFLNT.BAS. See sample output in Appendix B.

Table A-4. Contributions from antenna region 3 (shown in Fig. A-1).[a]

Horn gain, dBi	α_{A3} (see Table A-1)	T_p, K	Calculated ΔT_{A3}, K	Measured ΔT_{A3},[b] K	Difference, K
29.7	0.0022	298.6	0.657	0.41	0.25
28.7	0.0017	300.1	0.510	0.39	0.12
26.9	0.0011	298.8	0.329	0.31	0.02
25.1	0.0007	299.8	0.210	0.26	−0.05
22.5	0.0004	300.0	0.120	0.30	−0.18

[a] Based on the 243.8-cm-diameter BWG opening.
[b] See Table 5.

Table A-5. Contributions from horn region 2 (shown in Fig. A-1).[a]

Horn gain, dBi	8.7 deg		68.2 deg		ΔT_{A4},[c] K	α_{H2}[d]
	$\sum T_{Ai}$,[b] K	η_B[b]	$\sum T_{Ai}$,[b] K	η_B[b]		
29.7	4.4081	0.9736	4.5288	0.99998	0.1207	0.0264
28.7	4.3238	0.9573	4.5182	0.99997	0.1944	0.0427
26.9	4.2223	0.9329	4.5289	0.99995	0.3066	0.0671
25.1	3.9745	0.8768	4.5384	0.99997	0.5639	0.1231
22.5	3.1458	0.6946	4.5419	0.9997	1.3961	0.3051

[a] Horn radiation between subreflector edge (8.7 deg) and main reflector edge (68.2 deg).
[b] The values for $\sum T_{Ai}$ and η_B were obtained from the TYO61M4A program. See Appendix B for a sample case printout.
[c] $\Delta T_{A4} = \sum T_{Ai}$ at 68.2 deg $- \sum T_{Ai}$ at 8.7 deg.
[d] $\alpha_{H2} = \eta_B$ at 68.2 deg $- \eta_B$ at 8.7 deg.

Table A-6. Contributions for horn region 3 spillover losses (see Fig. A-1).

Horn gain, dBi	α_{H3} (see Table A-1)	$(\overline{T_b})_{H3}$, K	ΔT_{A5}, K
29.7	0.0030	6.0	0.018
28.7	0.0076	6.0	0.046
26.9	0.0156	6.0	0.094
25.1	0.0234	6.0	0.140
22.5	0.0386	6.0	0.232

Appendix B

Sample Printouts of Computer Programs Used to Compute Antenna Temperature Contributions

I. Program TYO61M4A.FOR (Only partial printout shown)

PROGRAM TYO61M4A.FOR
BY T. OTOSHI
LATEST REVISION: JUNE 30, 1993

PROGRAM TO COMPUTE ANTENNA GAIN AND ANTENNA
TEMPERATURE FROM PATTERN DATA
AND BRIGHTNESS TEMPERATURE DATA
THAT IS EITHER READ IN OR GENERATED BY PROGRAM

DATE OF THIS RUN: 3-15-94

OUTPUT FILENAME: OUTDAT\29_8DBNC.OD1

ANT PATTERN FILENAME: PAT\19_034M.PAT

BRIGHTNESS TEMPERATURES ARE GENERATED BY THIS PROGRAM

BRIGHTNESS TEMP PARAMETER FILENAME: NBTP\19_034.BT1

29.7 DBI CORR HORN PATTERN AT 8.450 GHZ FROM P.LEE 5/26/93
X-BAND AT F1, 29.8 DB HORN, NO CELOTEX, 14SEP 1993, 8.45 GHZ

ANTENNA BEAM EFFICIENCY, TEMPERATURE, AND GAIN E AND H PLANE PATTERN CASE

I	THETAI (DEG)	F1 (DB)	F2 (DB)	TBI (DEG K)	ETAI	SUM ETAI	TAI (DEG K)	SUMTAI (DEG K)	THETAL (DEG)
					ZENITH VALUE				
1	.0	.0	.0	4.523	.000000	.000000	.000000	.000000	.5
2	1.0	-.4	-.3	4.524	.137819	.137819	.623431	.623431	1.5
3	2.0	-1.4	-1.4	4.524	.215778	.353597	.976212	1.599643	2.5
4	3.0	-3.2	-3.2	4.526	.214926	.568524	.972756	2.572399	3.5
5	4.0	-5.7	-5.6	4.528	.162605	.731129	.736249	3.308648	4.5
6	5.0	-8.7	-8.6	4.531	.102488	.833617	.464366	3.773014	5.5
7	6.0	-11.7	-11.6	4.534	.061269	.894886	.277796	4.050810	6.5
8	7.0	-14.2	-14.2	4.538	.039816	.934702	.180700	4.231510	7.5
9	8.0	-16.5	-16.4	4.543	.027227	.961929	.123685	4.355195	8.5
	8.7 deg								
10	9.0	-19.2	-18.9	4.548	.016613	.978541	.075560	4.430755	9.5
11	10.0	-22.8	-22.3	4.554	.008287	.986829	.037739	4.486494	10.5
12	11.0	-26.3	-26.0	4.561	.003995	.990823	.018220	4.486713	11.5
13	12.0	-28.1	-28.0	4.568	.002782	.993605	.012709	4.499422	12.5
14	13.0	-29.4	-29.1	4.576	.002284	.995890	.010454	4.509876	13.5
15	14.0	-32.0	-31.3	4.585	.001413	.997303	.006478	4.516354	14.5
16	15.0	-36.1	-35.2	4.594	.000609	.997912	.002797	4.519151	15.5
17	16.0	-38.1	-38.4	4.604	.000354	.998265	.001629	4.520780	16.5
18	17.0	-37.6	-38.0	4.615	.000415	.998681	.001918	4.522697	17.5
19	18.0	-38.8	-38.3	4.627	.000372	.999053	.001719	4.524417	18.5
20	19.0	-42.5	-41.1	4.639	.000186	.999239	.000864	4.525280	19.5

21	20.0	-46.7	-45.8	4.652	.000070	.999309	.000328	4.525609	20.5
22	21.0	-44.8	-45.8	4.667	.000091	.999400	.000426	4.526034	21.5
23	22.0	-44.0	-44.1	4.681	.000126	.999527	.000592	4.526627	22.5
24	23.0	-46.4	-45.0	4.697	.000091	.999618	.000427	4.527054	23.5
25	24.0	-51.9	-49.1	4.714	.000033	.999650	.000154	4.527207	24.5
26	25.0	-51.7	-53.3	4.732	.000020	.999671	.000097	4.527304	25.5
27	26.0	-48.6	-50.1	4.750	.000044	.999715	.000208	4.527513	26.5
28	27.0	-48.9	-48.8	4.770	.000051	.999765	.000242	4.527754	27.5
29	28.0	-52.6	-50.6	4.790	.000028	.999794	.000136	4.527891	28.5
30	29.0	-58.9	-55.9	4.812	.000008	.999802	.000039	4.527929	29.5
31	30.0	-54.9	-57.9	4.834	.000010	.999812	.000050	4.527979	30.5
32	31.0	-52.3	-53.7	4.859	.000022	.999835	.000109	4.528088	31.5
33	32.0	-53.2	-52.8	4.884	.000023	.999858	.000112	4.528200	32.5
34	33.0	-57.4	-55.0	4.911	.000012	.999869	.000057	4.528257	33.5
35	34.0	-61.9	-61.1	4.938	.000003	.999873	.000017	4.528275	34.5
36	35.0	-57.2	-62.1	4.968	.000006	.999879	.000031	4.258305	35.5
37	36.0	-55.1	-57.1	4.998	.000013	.999892	.000064	4.258368	36.5
38	37.0	-55.9	-55.9	5.031	.000013	.999905	.000067	4.258435	37.5
39	38.0	-60.0	-57.5	5.064	.000007	.999912	.000037	4.258472	38.5
40	39.0	-68.2	-62.6	5.101	.000002	.999914	.000010	4.258482	39.5
41	40.0	-62.6	-68.1	5.137	.000002	.999916	.000010	4.528492	40.5
42	41.0	-58.9	-61.8	5.178	.000005	.999921	.000028	4.528520	41.5
43	42.0	-58.7	-59.2	5.218	.000007	.999929	.000038	4.528559	42.5
44	43.0	-61.2	-59.4	5.263	.000006	.999934	.000029	4.528588	43.5
45	44.0	-67.2	-62.4	5.308	.000002	.999937	.000012	4.528600	44.5
46	45.0	-67.4	-69.3	5.357	.000001	.999938	.000005	4.528605	45.5
47	46.0	-62.1	-69.5	5.407	.000002	.999940	.000012	4.528617	46.5
48	47.0	-60.0	-63.6	5.462	.000004	.999944	.000025	4.528642	47.5
49	48.0	-60.1	-61.6	5.517	.000005	.999950	.000029	4.528671	48.5
50	49.0	-62.2	-61.8	5.578	.000004	.999954	.000023	4.528694	49.5
51	50.0	-66.5	-64.1	5.640	.000002	.999956	.000011	4.528706	50.5
52	51.0	-69.5	-69.2	5.709	.000001	.999956	.000004	4.528710	51.5
53	52.0	-65.6	-75.8	5.777	.000001	.999958	.000006	4.528716	52.5
54	53.0	-62.8	-69.1	5.854	.000002	.999960	.000013	4.528728	53.5
55	54.0	-61.9	-65.5	5.931	.000003	.999963	.000019	4.528748	54.5
56	55.0	-62.3	-64.4	6.018	.000003	.999966	.000020	4.528768	55.5
57	56.0	-64.2	-64.9	6.106	.000002	.999969	.000015	4.528783	56.5
58	57.0	-67.6	-67.2	6.204	.000001	.999970	.000008	4.528791	57.5
59	58.0	-73.2	-71.9	6.303	.000000	.999970	.000003	4.528973	58.5
60	59.0	-75.2	-80.9	6.416	.000000	.999971	.000001	4.528794	59.5
61	60.0	-70.9	-74.5	6.529	.000000	.999971	.000003	4.528797	60.5
62	61.0	-68.6	-69.4	6.658	.000001	.999972	.000006	4.528803	61.5
63	62.0	-67.9	-67.1	6.788	.000001	.999973	.000009	4.528812	62.5
64	63.0	-68.5	-66.2	6.938	.000001	.999975	.000010	4.528822	63.5
65	64.0	-70.3	-66.4	7.089	.000001	.999976	.000009	4.528831	64.5
66	65.0	-73.3	-67.5	7.265	.000001	.999977	.000006	4.528837	65.5
67	66.0	-76.3	-69.6	7.442	.000001	.999977	.000004	4.528841	66.5
68	67.0	-75.0	-73.2	7.651	.000000	.999978	.000002	4.528843	67.5
69	68.0	-71.7	-79.9	7.860	.000000	.999978	.000002	4.528846	68.5
	68.2 deg								
70	69.0	-69.3	-89.3	8.111	.000000	.999979	.000004	4.528850	69.5
71	70.0	-67.7	-77.9	8.363	.000001	.999979	.000006	4.528856	70.5
72	71.0	-66.8	-73.4	8.671	.000001	.999980	.000009	4.528865	71.5
73	72.0	-66.3	-71.0	8.979	.000001	.999982	.000011	4.528876	72.5
74	73.0	-66.2	-69.7	9.363	.000001	.999983	.000013	4.528890	73.5
75	74.0	-66.3	-69.0	9.748	.000001	.999985	.000014	4.528904	74.5

II. Program SREFLNT1.BAS
(Only partial printout shown)

PROGRAM ID: SREFLNT1.BAS
WRITTEN BY TOM OTOSHI LAST REV: MARCH 14, 1994

DATE OF THIS RUN: 3-22-93

CASEID THIS RUN: 29.8_DBI HORN NO CELOTEX 14SEP93 MEAS AT F1

FINAL REDUCED DATA

DBEFF = DELTA BEAM EFFICIENCY AT ANGLE THETA
TBI = INTERPOLATED BRIGHTNESS TEMP
DTA = DELTA ANTENNA TEMPERATURE
CUMTA = CUMULATIVE ANTENNA TEMP

THETA (DEG)	DBEFF	TBI (K)	DTA (K)	CUMTA (K)
72.8205	0.000400	226.922	0.0908	0.0908
73.2500	0.000400	224.986	0.0900	0.1808
73.7500	0.000300	222.650	0.0688	0.2476
74.2500	0.000200	220.080	0.0440	0.2916
74.7500	0.000100	217.277	0.0217	0.3133
75.2500	0.000200	214.475	0.0429	0.3562
75.7500	0.000000	211.672	0.0000	0.3562
76.2500	0.000100	208.588	0.0209	0.3771
76.7500	0.000100	205.223	0.0205	0.3976
77.2500	0.000000	201.857	0.0000	0.3976
77.7500	0.000100	198.492	0.0199	0.4175
78.2500	0.000000	194.792	0.0000	0.4175
78.7500	0.000000	190.756	0.0000	0.4175
79.2500	0.000100	186.719	0.0187	0.4361
79.7500	0.000000	182.683	0.0000	0.4361
80.2500	0.000000	178.256	0.0000	0.4361
80.7500	0.000000	173.439	0.0000	0.4361
81.2500	0.000000	168.621	0.0000	0.4361
81.7500	0.000100	163.804	0.0164	0.4525
82.2500	0.000000	158.564	0.0000	0.4525
82.7500	0.000000	152.903	0.0000	0.4525
83.2500	0.000000	147.241	0.0000	0.4525
83.7500	0.000000	141.580	0.0000	0.4525
84.2500	0.000000	135.637	0.0000	0.4525
84.7500	0.000000	129.412	0.0000	0.4525
85.2500	0.000100	123.096	0.0123	0.4648
85.7500	0.000000	116.688	0.0000	0.4648
86.2500	0.000000	110.398	0.0000	0.4648
86.7500	0.000000	104.225	0.0000	0.4648
87.2500	0.000000	98.671	0.0000	0.4648
87.7500	0.000000	93.735	0.0000	0.4648
88.2500	0.000000	90.554	0.0000	0.4648
88.7500	0.000000	89.128	0.0000	0.4648

C-3

89.2500	0.000000	91.331	0.0000	0.4648
89.7500	0.000000	97.162	0.0000	0.4648
90.2500	0.000000	91.778	0.0000	0.4648
90.7500	0.000000	75.179	0.0000	0.4648
91.2500	0.000000	61.955	0.0000	0.4648
91.7500	0.000000	52.109	0.0000	0.4648
92.2500	0.000000	44.342	0.0000	0.4648
92.7500	0.000000	38.655	0.0039	0.4687
93.2500	0.000000	34.057	0.0000	0.4687
93.7500	0.000000	30.547	0.0000	0.4687
94.2500	0.000000	27.626	0.0000	0.4687
94.7500	0.000000	25.294	0.0000	0.4687
95.2500	0.000000	23.305	0.0000	0.4687
95.7500	0.000000	21.659	0.0000	0.4687
96.2500	0.000000	20.298	0.0000	0.4687
96.7500	0.000000	19.222	0.0000	0.4687
97.2500	0.000000	18.145	0.0000	0.4687
97.7500	0.000000	17.069	0.0000	0.4687
98.2500	0.000000	16.197	0.0000	0.4687
98.7500	0.000000	15.529	0.0000	0.4687
99.2500	0.000000	14.860	0.0000	0.4687
99.7500	0.000000	14.192	0.0000	0.4687

TOTAL COMPUTED ANTENNA TEMP = 0.469 K

SUM OF DELTA BEAM EFF FOR GROUND REGION ONLY = 0.00220
SUM OF DELTA BEAM EFF FOR GROUND + SKY REGION = 0.00230

SUBREFL EFF RELATIVE TO HORN INPUT = 0.970600
SUBREFL EFF × ANT TEMP CONTRIBUTION = 0.455 K
